Journal of Inorganic Biochemistry 104 (2010) 1171–1177

Contents lists available at ScienceDirect

Journal of Inorganic Biochemistry

journal homepage: www.elsevier.com/locate/jinorgbio

Mo(II) complexes: A new family of cytotoxic agents?

Daniel Bandarra [a], Miguel Lopes [a], Telma Lopes [a], Joana Almeida [a], Marta S. Saraiva [a], Maria Vasconcellos-Dias [a], Carla D. Nunes [a], Vitor Félix [b], Paula Brandão [c], Pedro D. Vaz [a], Margarida Meireles [a,*], Maria José Calhorda [a]

[a] Departamento de Química e Bioquímica, CQB, Faculdade de Ciências, Universidade de Lisboa, Campo Grande 1749-016 Lisboa, Portugal
[b] Departamento de Química, CICECO and Secção Autónoma de Ciências da Saúde, Universidade de Aveiro, 3810-193 Aveiro, Portugal
[c] Departamento de Química, CICECO, Universidade de Aveiro, 3810-193 Aveiro, Portugal

ARTICLE INFO

Article history:
Received 12 May 2010
Received in revised form 5 July 2010
Accepted 6 July 2010
Available online 17 July 2010

Keywords:
Molybdenum
1,10-Phenanthroline
Antitumor activity
X-ray structure
Interaction with DNA

ABSTRACT

Several molybdenum complexes, $[Mo(\eta^3\text{-}C_3H_5)X(CO)_2(N\text{-}N)]$ (N-N = 1,10-phenanthroline, phen: X = CF_3SO_3 **T1**, X = Br **B1**, X = Cl **C1**; N-N = 2,2′-bipyridyl, X = CF_3SO_3 **T2**, X = Br **B2**) and $[W(\eta^3\text{-}C_3H_5)Br(CO)_2(phen)]$ (**W1**) have been synthesized and characterized. Their antitumor properties have been tested *in vitro* against human cancer cell lines cervical carcinoma (HeLa) and breast carcinoma (MCF-7) using a metabolic activity test (3-(4,5-dimethylthiazol-2-yl)-2,5-diphenyltetrazolium bromide, MTT), leading to IC_{50} values ranging from 3 to 45 μM, approximately. Most complexes exhibited significant antitumoral activity. Complexes **B1** and **T2** were chosen for subsequent studies aiming to understand their mechanism of action. Cellular uptake of molybdenum and octanol/water partition assays revealed that both **B1** and **T2** exhibit a selective uptake by cells and intermediate partition coefficients. The binding constants of **B1** and **T2** with ct DNA, as determined by absorption titration, are 2.08 $(\pm 0.98)\times 10^5$ and 3.68 $(\pm 2.01)\times 10^5\ M^{-1}$, respectively. These results suggest that they interact with DNA changing its conformation and possibly inducing cell death, and may therefore provide a valuable tool in cancer chemotherapy.

1. Introduction

Organometallic complexes play a major role in many fields of chemistry, as precursors to new materials [1–3], in catalysis [4,5] and in applications to medicine [6,7]. Their versatility is associated with the possibility of finely tuning the stereoelectronic properties of metal centers by changing ligands, oxidation state and electronic configuration.

In the last decades, after the success of *cis*-platin, *cis*-$[PtCl_2(NH_3)_2]$, as antitumor agent [8], the interest in the use of transition metal complexes in medicine has grown rapidly. In particular, the search for new compounds that could overcome cell resistance and toxicity problems associated with platinum complexes led to the study of other metal containing antitumor drugs. In 1979, Köpf and Köpf-Maier reported the antitumor action of several metal-based complexes with Ti, V, Nb, Mo and Re [9], and later, several researchers reported interesting anticancer activities for neutral and charged metallocene derivatives, amplifying the number of possible clinically useful drugs [10–14].

A number of molybdenum containing molecules have since then been described to display cancerostatic activity. These include Na_2MoO_4 [15], molybdenum alone [16], heteropolyacid Mo salts [17], polyoxomolybdates [18], and Mo complexes bound to small carborane ligands and chiral octahedral complexes [19,20]. Portuguese researchers in 2005 studied several molybdenum(II) compounds, concluding that they were very efficient cytotoxic agents against six cell lines, and filed a patent [21]. Since molybdenum is an essential trace metal for organisms, plays a crucial role as cofactor for important enzymes [22], and is transported and excreted as the anion $[MoO_4]^{2-}$, its low toxicity and its effects on metabolism should make possible the use of complexes of this metal as therapeutic agents. The mechanisms of action of most of the organometallic complexes of molybdenum are far from being understood. Since cell growth is slowed down by those compounds, it seems conceivable that the inhibitory activity might in some way be related to DNA damage. This can be due to a direct action on the DNA molecule (e.g. intercalation in the double helix) or by the oxidative action of oxygen free radicals generated by the chemical agents.

We reported in an earlier work the antitumor activity of Mo(II) complexes associated with ferrocene, but the results were disappointing [23], even though the ferricinium ion by itself and other derivatives display some activity [24]. On the other hand, complexes $[Mo(\eta^3\text{-}C_3H_5)X(CO)_2(N\text{-}N)]$, with X = Br, CF_3SO_3 and N-N = 2-(2′-pyridyl)benzimidazole) or 2-(2′-pyridyl)imidazole) exhibited a high activity against several cell lines [25]. In this study, we describe the noticeable antitumor activity of a family of 2,2′-bipyridyl and 1,10-

* Corresponding author. Tel.: +351 217500923; fax: +351 217500088.
E-mail address: mmmeireles@fc.ul.pt (M. Meireles).

0162-0134/$ – see front matter © 2010 Elsevier Inc. All rights reserved.
doi:10.1016/j.jinorgbio.2010.07.006

phenanthroline molybdenum complexes with halide and triflate counter-anions, and perform a series of biological studies in order to provide new insights on the mechanisms of action of these compounds.

2. Experimental

2.1. Materials

Commercially available reagents and all solvents were purchased from standard chemical suppliers. Molybdenum hexacarbonyl and 2,2′-bipyridyl were purchased from Fluka, allyl bromide from Sigma-Aldrich, 1,10-phenanthroline 1-hydrate from Panreac, and octanol from Riedel-de Haën, Germany. The RPMI 1640 cell culture medium, fetal bovine serum (FBS) were purchased from LONZA Co. MTT (3-(4,5-dimethylthiazol-2-yl)-2,5-diphenyl tetrazolium bromide) was purchased from Sigma Chemical Co, USA. Solvents were dried using common procedures. Dichloromethane was distilled over CaH_2, and n-hexane over Na/benzophenone, under nitrogen. The syntheses of the complexes were carried out under nitrogen atmosphere using Schlenk tube techniques. The complexes [MoBr(η^3-C_3H_5)(CO)$_2$(CH_3CN)$_2$], [MoBr(η^3-C_3H_5)(CO)$_2$(N-N)] (N-N = 2,2′-bipyridyl, bpy; 1,10-phenanthroline, phen), [MoCl(η^3-C_3H_5)(CO)$_2$(phen)] [26] and [W(η^3-C_3H_5)Br(CO)$_2$(phen)] [27] were synthesized according to literature procedures. Calf thymus DNA (ct DNA) was purchased from Sigma Chemical Co. Ltd. and a stock solution was prepared by dilution in a buffer solution (50 mM NaCl/5 mM Tris–HCl, pH 7.1) followed by stirring at 4 °C for two days. This solution was stored at 4 °C. The stock solution of ct DNA gave a ratio of UV absorbance at 260 and 280 nm (A_{260}/A_{280}) of 1.87, indicating that the DNA was sufficiently free of protein contamination. The DNA concentration was determined by the UV absorbance at 260 nm after 1:10 dilution using $\varepsilon = 6600\ M^{-1}\ cm^{-1}$ [23]. MTT was dissolved (5 mg/mL) in phosphate buffer saline pH 7.2.

2.2. Methods

Infrared spectra were measured on a Nicolet 6700 spectrometer. Samples were run as KBr pellets. The intensity of reported IR signals is defined as s = strong, m = medium, and w = weak. NMR spectra were recorded on a Bruker Avance-400 spectrometer in $CDCl_3$ or deuterated DMSO. The splitting of proton resonances in the reported ^{1}H NMR spectra is defined as s = singlet, d = doublet, t = triplet, and m = multiplet. UV–Vis spectra were recorded on a Shimadzu UV-2450 equipped with a Peltier cell for temperature control. High-resolution mass spectrometry (HR-MS) measurements were accomplished using electrospray ionization technique (ESI). All experiments were performed on an ApexQe FTICR Mass Spectrometer from Bruker Daltonics equipped with a combined Apollo II electrospray/MALDI ion source and a 7 T actively shielded superconducting magnet. Samples were introduced at a flow rate of 120 μL/h into the ESI source using an infusion pump. The applied spray potential was 4.5 kV and the capillary temperature was set at 200 °C. All remaining parameters were optimized to ensure the highest abundance possible for the ions of interest. All MS data were acquired in the positive ion mode, the full scan spectra being recorded in the *m/z* 50–1200 range. MS^2 with collision induced dissociation (CID) experiments were performed with argon, and the collision energy was gradually increased until the precursor and the product ions could both be observed in the MS^2 spectrum, though the precursor peak intensity was reduced compared to its original relative intensity. Prior to all MS experiments a calibration step was performed with a 2.8×10^{-6} M solution of polyethylene glycol 200 (PEG200) in HPLC grade methanol acidified with 0.1% (v/v) of formic acid. All errors of measured *m/z* ions were found to be below 5 ppm compared to expected values.

2.3. Synthesis of molybdenum(II) complexes

2.3.1. [Mo(η^3-C_3H_5)(CF_3SO_3)(CO)$_2$(1,10-phenanthroline)] (**T1**)

Thallium triflate ($TlCF_3SO_3$) (0.353 g, 1 mmol) was added to a solution of [MoBr(η^3-C_3H_5)(CO)$_2$(1,10-phenanthroline)] (0,453 g, 1 mmol) in acetonitrile (20 mL), and the mixture was refluxed for 5 h. A white solid of TlBr was formed and filtered with celite. The solid was washed 3 times with acetonitrile. The filtrate was evaporated and the solid residue dissolved in dichloromethane. Addition of n-hexane resulted in the formation of red crystals after a few days.

Yield: 76% (0.397 g)

IR (KBr disc) (cm^{-1}): 3435 (m); 2068 (m); 1936 (vs); 1847 (vs); 1629 (m); 1604 (m); 1519 (m); 1479 (m); 1426 (m); 1319 (s); 1311 (s); 1237 (s); 1204 (s); 1180 (vs); 1014 (s); 956 (w); 930 (w); 851 (s); 780 (m); 725 (s); 632 (s); 580 (m); 522 (m); 493 (w).

^{1}H NMR (400 MHz, DMSO-d_6): δ 1.39 (d, H_{anti}); 3.50 (d, H_{syn}); 3.79 (d, H_{syn}); 4.22 (m, H_{meso}); 8.06 (m, H_7); 8.22 (s, H_4/H_5); 8.34 (s, H_2); 8.80 (d, H_6); 8.88 (d, H_3); 9.37 (d, H_8); 9.50 (s, H_1).

HR–ESI–MS (*m/z*): calcd for $[C_{17}H_{13}N_2O_2Mo]^+$, 375.00289; obsd, 375.00299; error, + 0.3 ppm.

2.3.2. [Mo(η^3-C_3H_5)(CF_3SO_3)(CO)$_2$(2,2′-bipyridyl)] (**T2**)

Thallium triflate ($TlCF_3SO_3$) (0.353 g, 1 mmol) was added to a solution of [MoBr(η^3-C_3H_5)(CO)$_2$(2,2′-bipyridyl)] (0,429 g, 1 mmol) in acetonitrile (20 mL), and the mixture was refluxed for 5 h. A white solid of TlBr was formed and filtered with celite. The solid was washed 3 times with acetonitrile. The filtrate was evaporated and the solid residue dissolved in dichloromethane. Addition of n-hexane resulted in the formation of red crystals after a few days.

Yield: 72% (0.359 g)

IR (KBr disc) (cm^{-1}): 3436 (m); 3069 (m); 1947 (vs); 1863 (vs); 1602 (s); 1573 (m); 1495 (m); 1474 (s); 1441 (s); 1389 (w); 1312 (s); 1302 (s); 1287 (s); 1237 (s); 1219 (s); 1174 (s); 1158 (s); 1127 (w); 1109 (w); 1077 (m); 1034 (s); 930 (m); 795 (m); 764 (s); 734 (s); 657 (w); 650 (w); 630 (s); 577 (m); 570 (m); 516 (m); 504 (m); 439 (m); 418 (m).

^{1}H NMR (400 MHz, DMSO-d_6): δ 1.63 (d, H_{anti}); 3.76 (d, H_{syn}); 4.06 (m, H_{meso}); 7.69 (t, H_3/H_6); 8.08 (t, H_2/H_7); 8.16 (d, H_4/H_5); 9.2 (s, H_1/H_8).

HR–ESI–MS (*m/z*): calcd for $[C_{15}H_{13}N_2O_2Mo]^+$, 351.00285; obsd, 351.00315; error, + 0.9 ppm.

2.4. Crystallography

X-ray single crystal data of [Mo(η^3-C_3H_5)(CF_3SO_3)(CO)$_2$(1,10-phenantroline)] (**T1**) and [Mo(η^3-C_3H_5)(CF_3SO_3)(CO)$_2$(2,2′-bipyridyl)] (**T2**) were collected on a CCD Bruker APEX II at 150(2) K using graphite monochromatized Mo-Kα radiation (λ = 0.71073 Å).

The selected crystal was positioned at suitable distance from the CCD, 45 mm for **T1** and 35 mm for **T2**, and the corresponding spots were measured with counting time of 60 s for **T1** and 10 s for **T2.** Data reductions were carried out with SAINT-NT suite from Bruker AXS. Data of both complexes were corrected for absorption effects through the multi-scan method using the same software. The structures were solved with the SHELXS and refined by full-matrix least squares with the SHELXL-97 program using the SHELX97 software package [28]. All non-hydrogen atoms were refined with anisotropic thermal parameters. The hydrogen atoms were introduced in the structure refinement with individual isotropic temperature factors equal 1.2 times to those they are attached. The final *R* values obtained for complexes **T1** and **T2** together with pertinent crystallographic data are summarized in Table 1. Molecular diagrams were drawn with PLATON [29].

2.5. Physical measurements

2.5.1. Cell cultures

HeLa (cervical carcinoma) and MCF-7 (breast carcinoma) cell lines were maintained in RPMI 1640, while N1E-115 (neuroblastoma) cells

Table 1
Pertinent crystallographic data for complexes [Mo(η^3-C_3H_5)(CF_3SO_3)$(CO)_2$(phen)] (**T1**) and [Mo(η^3-C_3H_5)(CF_3SO_3)$(CO)_2$(bpy)] (**T2**).

Complex	T1	T2
Molecular formula		
[Mo(η^3-C_3H_5)(CF_3SO_3)$(CO)_2$(N-N)]	N-N = phen	N-N = bpy
Empirical formula	$C_{18}H_{13}F_3MoN_2O_5S$	$C_{16}H_{13}F_3MoN_2O_5S$
M_w	522.30	498.28
Crystal system	Monoclinic	Monoclinic
Space group	$P2_1/c$	$P2_1/c$
a/[Å]	6.6085(2)	14.3395(7)
b/[Å]	17.0355(6)	9.7660(5)
c/[Å]	33.1497(10)	13.9669(7)
β/[°]	93.834(2)	115.249(2)
V/[Å^3]	3723.6(2)	1769.05(15)
Z	8	4
D_c [Mg m^{-3}]	1.863	1.871
μ/[mm^{-1}]	0.882	0.923
Reflections collected	11509	4566
Unique reflections, [R_{int}]	8767 [0.0520]	4108 [0.0288]
Final *R* indices		
R_1, wR_2 [$I>2\sigma I$]	0.0389, 0.0818	0.0246, 0.0647
R_1, wR_2 (all data)	0.0616, 0.0925	0.0285, 0.0667

were grown in DMEM. Both media were supplemented with 10% FBS, 200 U/mL penicillin, 100 μg/mL streptomycin and 0.3 g/mL L-glutamine in a humidified atmosphere of 95% air/5% CO_2 at 37 °C.

2.5.2. Cytotoxicity assay by MTT

The MTT assay was used to determine the cell viability as an indicator for the sensitivity of the cells to the complexes [Mo(η^3-C_3H_5)X$(CO)_2$(N-N)] (N-N = 1,10-phenanthroline: X = CF_3SO_3 **T1**, X = Br **B1**, X = Cl **C1**; N-N = 2,2′-bipyridyl, X = CF_3SO_3 **T2**, X = Br **B2**) and [W(η^3-C_3H_5)Br$(CO)_2$(phen)] (**W1**).

Exponentially growing cells were seeded at a density of approximately 4×10^5 cells/mL, in a 96-well flat-bottomed microplate, and 48 h later they were treated with the complexes. The complexes were dissolved in DMSO and tested in concentrations ranging from 1 to 1000 μM. For the kinetic studies, cell cultures were exposed to different concentrations of compounds for different periods of time (1, 2, 24, and 48 h), after which the medium with the drug was removed and was replaced by fresh medium. Each experiment included ten replicates for the different concentrations of complexes and results represent at least 3 independent experiments. UV–Vis spectra of solutions with appropriate concentrations were measured during this period and showed no decomposition of the complexes being studied. Cytotoxicity of test compounds was evaluated by the MTT method [30]. The optical density was measured at 570 nm using a 96-well multiscanner autoreader. The IC_{50} were calculated by nonlinear regression analysis using the graphed Prism software (GRAFHPAD Software, Inc., San Diego, California).

2.5.3. Cellular uptake studies

HeLa cells were seeded in 100 mm dishes at 4×10^5 cells/mL and cultures were exposed to compounds in final concentrations of 0, 10, 50 and 100 μM for 48 h. Following treatment, cell cultures were trypsinized as described [31], and sedimented. The Mo content of cells was determined by inductively coupled plasma mass spectrometry (ICP-MS) by standard protocol at the University of Vigo, Spain.

2.5.4. Octanol/water partition coefficient

Water-saturated octanol and octanol-saturated water were prepared by shaking equal volumes of octanol and water for 5 h and allowing the mixture to separate into the respective phases for 24 h. Twenty micromolar solutions of complexes **T2** and **B1** were prepared in water-saturated octanol and their absorbance was analyzed by UV spectrophotometry. Three and six milliliters of drug solution were then added to 40 mL of octanol-saturated water. These solutions were shaken vigorously for 2 h. The aqueous phase was separated ensuring that there was no contamination from the octanol phase, and each of these solutions was analyzed by UV spectrophotometry to obtain the absorbance of the compounds.

2.5.5. Interaction of complexes with DNA

Calf thymus DNA (ctDNA) solutions of various concentrations (0–100 μM) were added to 20 μM buffered solutions (5 mM Tris, 50 mM NaCl, pH 7.2) of the metal complexes. The same amount of ctDNA solution was added to the reference cell in order to correct for the contribution of the increasing DNA concentration. Absorption spectra were recorded after equilibration at 37.0 °C for 10 min. The intrinsic binding constant, *K*, was determined from a plot of $D/\Delta\varepsilon_{ap}$ vs. *D* according to Eq. (1) [32]

$$D / \Delta\varepsilon_{ap} = D / \Delta\varepsilon + 1 / (\Delta\varepsilon \times K) \quad (1)$$

where *D* is the concentration of DNA in base pairs, $\Delta\varepsilon_{ap} = |\varepsilon_A - \varepsilon_F|$; $\varepsilon_A = A_{obs}$/[complex], and $\Delta\varepsilon = |\varepsilon_B - \varepsilon_F|$, with ε_B and ε_F corresponding to the extinction coefficient of the DNA-bound complex and unbound complex, respectively.

3. Results and discussion

3.1. Synthesis and spectroscopic studies

Complexes [Mo(η^3-C_3H_5)X$(CO)_2$(N-N)] (N-N = 1,10-phenanthroline: X = CF_3SO_3 **T1**, X = Br **B1**, X = Cl **C1**; N-N = 2,2′-bipyridyl, X = CF_3SO_3 **T2**, X = Br **B2**), depicted in Fig. 1, and [W(η^3-C_3H_5)Br$(CO)_2$(phen)] (**W1**) were synthesized in order to study their biological activity *in vitro*. All the complexes with X = Br were obtained directly from reaction between [MBr(η^3-C_3H_5)$(CO)_2(CH_3CN)_2$] (M = Mo, [26]W, [27]) and the diimine ligand, which led to the substitution of the two nitrile ligands (similarly for X = Cl). Reaction of [Mo(η^3-C_3H_5)Br$(CO)_2$(N-N)] with Tl[CF_3SO_3] in CH_3CN resulted in loss of the halide and coordination of the triflate ion, as reported for other complexes [25]. The triflate complexes **T1** and **T2** were structurally characterized by single crystal X-ray diffraction (see 3.2).

The FTIR spectra of **T1** showed the two strong typical bands assigned to the $\nu_{C\equiv O}$ stretching modes of the *cis* carbonyl ligands at 1936 and 1847 cm^{-1}, also observed at 1947 and 1864 for **T2**. Several bands characteristic of the coordinated triflate ion and the diimine ligand were also observed for both complexes.

The ^{1}H NMR spectrum of **T1** in deuterated DMSO displayed peaks of the 1,10-phenanthroline at 8.06 (H_7), 8.22 (H_4, H_5), 8.34 (H_2) 8.80 (H_6), 8.88 (H_3), 9.37 (H_8), and 9.50 ppm (H_1), reflecting the asymmetric coordination of the ligand, with one nitrogen trans to

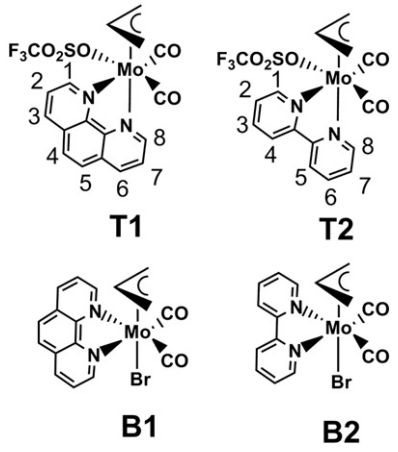

Fig. 1. Structures of complexes **T1–2**, **B1–2**, with numbering scheme.

the allyl and the second trans to one CO group (axial isomer). The allylic protons are observed at 1.39 (H_{anti}), 3.50 and 3.79 (H_{syn}), and 4.22 (H_{meso}) ppm in agreement with the presence of the axial isomer. The data for complex **T2** are analogous (see 2.3).

High-resolution mass spectra (HR-MS) were acquired using the electrospray ionization (ESI) technique to confirm the proposed structure of complexes **T1** and **T2**. Both the molecular mass and the isotopic pattern were analyzed. Although the ESI method is a very mild ionization technique, confirmation of the masses as formulated in Fig. 1, was not possible for both complexes **T1** and **T2**. The detected *m/z* peaks corresponded in both cases to the desired complexes with the loss of the CF_3SO_3 ligands.

Thus, complex **T1** has been successfully detected at *m/z* = 375.00299, making possible its formulation as $[\mathbf{T1}-CF_3SO_3]^+$, with an error of 0.3 ppm relative to the expected ion at *m/z* = 375.00289, which is in extremely good agreement. Collision induced dissociation (CID) experiments with argon revealed the loss of both CO ligands. This afforded an ion at *m/z* = 319.01304 formulated as $[\mathbf{T1}-2CO-CF_3SO_3]^+$, showing an error of 0.1 ppm relative to the expected ion at *m/z* = 319.01302. Another species was also detected at *m/z* = 365.01876 and was positively identified as $[\mathbf{T1}-C_3H_5-CF_3SO_3+CH_3O]^+$. It probably arose from the exchange of the allyl ligand in the initial complex with methoxide, and shows an error of 4.8 ppm compared to the expected ion at *m/z* = 364.98212. This cation also loses both CO ligands originating an ion at *m/z* = 309.96370 corresponding to an oxidized species formulated as $[Mo(phen)O_2]^+$ (error of 2.9 ppm compared to the expected ion at *m/z* = 309.96366). This last species may be originated from gas-phase reactions with the solvent (methanol).

Complex **T2** was also detected as $[\mathbf{T2}-CF_3SO_3]^+$ at *m/z* = 351.00315. Compared to the expected mass at *m/z* = 351.00285, this represents an error of 0.9 ppm, in excellent agreement. CID experiments revealed the loss of both CO ligands, from $[\mathbf{T2}-CF_3SO_3]^+$ ion originating a species at *m/z* = 295.01363, as already described above for **T1**. This corresponds to a cation formulated as $[\mathbf{T2}-2CO-CF_3SO_3]^+$ with an error of 2.2 ppm relative to the expected ion at *m/z* = 295.01297.

3.2. Crystal structures

The crystal structures of complexes $[Mo(\eta^3\text{-}C_3H_5)(CF_3SO_3)(CO)_2(N\text{-}N)]$ with N-N = 1,10-phenanthroline (**T1**) and N-N = 2,2′-bipyridyl (**T2**) were determined by X-ray diffraction. Selected bond distances and angles in the molybdenum(II) coordination sphere of these two complexes are given in Table 2. The asymmetric unit of **T1** is composed of two discrete molecules (A and B) which exhibit identical distances and angles. Consequently average values will be used throughout the current text. The molecular structures found in the solid state are shown in Fig. 2 for **T1** (molecule A) and in Fig. 3 for **T2**. These two complexes display identical pseudo-octahedral coordination environments with the two nitrogen donors of the bidentate chelating ligand, phen in **T1** and bpy in **T2**, occupying axial and equatorial coordination positions, respectively. The remaining axial position is fulfilled with the centroid of the allyl ligand, which together with two *cis* carbonyl ligands defined a *fac* arrangement, consistent with the existence of the axial isomer in ^1H NMR solution studies (see above). In addition, the allyl ligand adopts the usual *endo* conformation relative to the two carbonyl ligands.

The equatorial Mo–O bond between the triflate anion and metal center intercepts the plane of the polypyridyl ligand at 75.6° in **T1** and 76.3° in **T2**. This geometric arrangement is equivalent to that observed in the related complex $[Mo(\eta^3\text{-}C_3H_5)(CF_3SO_3)(CO)_2(2\text{-}(2'\text{-pyridyl})benzimidazole)]$ [25], in which the Mo–OSO_2CF_3 bond makes with the 2-(2′-pyridyl)benzimidazole plane an angle of 79.1°. The Mo–O bond of 2.264(2) Å in **T1** is slightly longer than the corresponding one of 2.2394(15) Å in **T2**, which is similar to the observed in the quoted complex (2.233(5) Å). The complexes **T1** and **T2** display nearly identical Mo–N bond lengths and N–Mo–N angles, which are consistent with the identical coordination constraints imposed by phen and bpy ligands. In addition, these parameters, as well as the remaining ones listed in Table 2, agree well with those found for other related *fac*-$Mo(\eta^3\text{-}C_3H_5)(CO)_2$ polypyridyl complexes, although some of them exist as the equatorial isomer, as observed for $[Mo(\eta^3\text{-}C_3H_5)Br(CO)_2(N\text{-}N)]$, with N-N = 2,2′-bipyridyl (**B2**) or 1,10-phenanthroline (**B1**) [33–36].

Table 2
Selected bond lengths (Å) and angles (°) in the molybdenum coordination sphere of $[Mo(\eta^3\text{-}C_3H_5)(CF_3SO_3)(CO)_2(N\text{-}N)]$ complexes, with N-N = phen (**T1**) or bpy (**T2**).

Complex	T1		T2
Molecule	A	B	
Bond lengths			
Mo–allyl	2.197(3)–2.331(3)	2.199(3)–2.337(3)	2.2019(19)–2.341(2)
Mo–C(1)	1.957(3)	1.967(3)	1.959(2)
Mo–C(2)	1.939(3)	1.937(3)	1.946(2)
Mo–N(11)	2.270(2)	2.274(2)	2.2815(16)
Mo–N(21)	2.210(2)	2.211(2)	2.2027(16)
Mo–O(3)	2.264(2)	2.2716(19)	2.2394(15)
Bond angles			
C(1)–Mo–C(2)	80.40(12)	82.75(12)	79.65(8)
N(11)–Mo–N(21)	73.68(8)	73.82(8)	72.83(6)
O(3)–Mo–C(2)	171.09(10)	170.29(10)	169.64(7)
O(3)–Mo–C(1)	98.54(10)	97.91(9)	99.38(8)
O(3)–Mo–N(11)	79.89(7)	78.71(8)	79.52(6)
O(3)–Mo–N(21)	80.42(8)	80.39(8)	81.73(6)
C(1)–Mo–N(11)	166.50(10)	165.58(10)	168.03(7)
C(1)–Mo–N(21)	92.82(10)	91.81(10)	95.21(7)
C(2)–Mo–N(11)	99.05(10)	98.24(10)	99.25(7)
C(2)–Mo–N(21)	90.78(10)	89.90(10)	88.07(7)

3.3. Cytotoxic studies

The molybdenum complexes were assayed for cytotoxic activity against HeLa (cervical carcinoma), MCF-7 (breast carcinoma) and

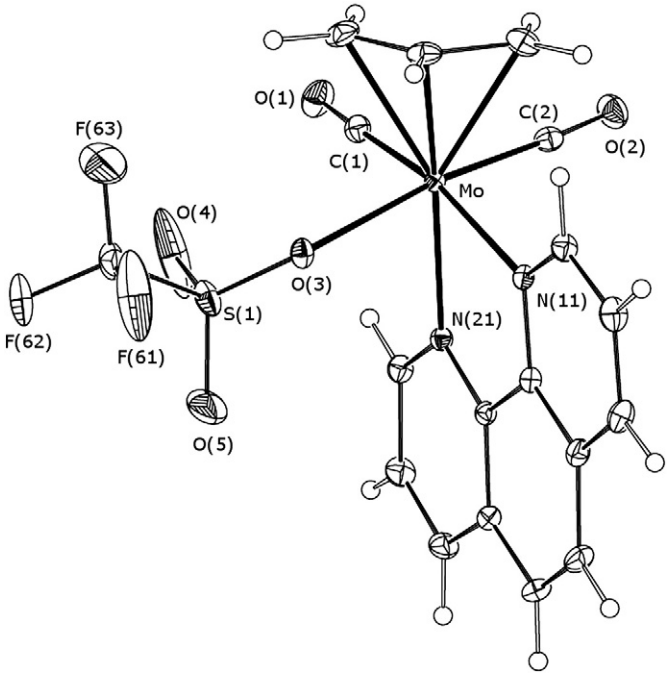

Fig. 2. Molecular structure of $[Mo(\eta^3\text{-}C_3H_5)(CF_3SO_3)(CO)_2(phen)]$ (**T1**) illustrated with the molecule A together with atomic notation scheme adopted for molybdenum, oxygen, fluorine, sulfur and nitrogen atoms. Thermal ellipsoids are drawn at the 30% probability level.

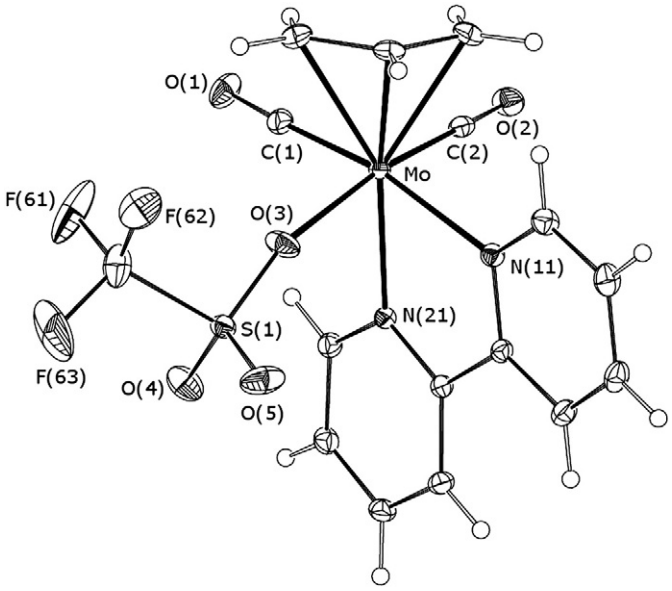

Fig. 3. Molecular structure of [Mo(η^3-C_3H_5)(CF_3SO_3)$(CO)_2$(bpy)] (**T2**). Remaining details as given in Fig. 2.

N1E-115 (neuroblastoma). These cells provide a readily available, easy to handle model cell line, against which all the complexes could be tested and compared. The cells were exposed to each of the compounds for a total of 48 h, to compare the results of the cell uptake experiments with the cytotoxicity. Using the colorimetric mitochondrial function-based MTT viability assay, the IC_{50} values (final concentration ≤0.5% DMSO) were calculated from dose–response curves obtained by nonlinear regression analysis. IC_{50} values are concentrations of drug required to inhibit tumor cell proliferation by 50%, compared to the control viability.

As demonstrated by the IC_{50} values listed in Table 3, all the molybdenum complexes, and to a smaller extent the tungsten complex, showed to be very effective as cytotoxic agents against the *in vitro* growth of various cancer cell lines. They exhibited activities with IC_{50} values ranging from 3 to 39 μM, approximately, in HeLa cells, 9 to 45 μM, approximately, in MCF-7 cells (except for **W1**, which showed less activity) and 4 to 60 μM approximately, in N1E-115 cells, with **T1** and **B1** being among the most potent. These results presented some interesting structure–activity relationships. All the complexes with 1,10-phenanthroline have comparable activity and achieved almost total inhibition (<10% cell viability) at the maximum concentration tested (1000 μM) for nearly all cell lines. In fact, its values are comparable to *cis*-platin, which has IC_{50} values below 10 μM with a range of cell lines [37,38]. It is interesting also to notice that the compounds with 2,2′-bipyridyl (**T2** and **B2**) also have comparable activities and showed a noteworthy cytotoxicity, although not as impressive as the previous ones. For further comparison between these two ligands, two complexes (**T2** and **B1**) have been chosen for complementary studies.

The effect of varying the total exposure time of cells to compounds **T2** and **B1** was also investigated. The dose–response curves for the treatment of HeLa cells with the compounds for 1, 2, 24, and 48 h are shown in Fig. 4 and the results of their cytotoxicity are summarized in Table 4. These results showed a decrease in the IC_{50} value of both complexes as the exposure time increases, although the difference between 24 h and 48 h does not seem relevant. This may be indicative that the maximum cytotoxic effect is established at 24 h of drug exposure time.

Table 3
In vitro cytotoxicity assays for molybdenum and tungsten complexes against HeLa, MCF-7, and N1E-115 cells (data are mean ± SD of three replicates each).

Compounds	IC_{50} (μM)		
	HeLa	MCF-7	N1E-115
T1	2.9 ± 0.004	13.4 ± 0.7	3.5 ± 1.0
T2	23.7 ± 0.005	44.5 ± 0.7	60.0 ± 0.4
B1	5.1 ± 1.0	8.9 ± 0.5	32.5 ± 1.3
B2	38.9 ± 7.9	30.6 ± 10.0	–
C1	8.2 ± 0.8	9.3 ± 0.6	6.7 ± 1.5
W1	12.8 ± 0.5	294.6 ± 1.4	4.6 ± 2.1

3.4. Cellular uptake studies

The intracellular Mo content was determined after treatment of HeLa cells with compounds **T2** and **B1**, in order to figure out the effect of altering the ligands on Mo cell uptake. The correlation of the Mo cell uptake with the cytotoxicity also provides information regarding the intracellular cytotoxic potential of complexes. Each compound was tested at three different concentrations (10, 50 and 100 μM). These concentrations were chosen based on the cytotoxicity data reported previously. The intracellular Mo concentration for the treated cells is shown in Fig. 5.

The intracellular molybdenum levels of the cells treated with **B1** revealed a significant increase, contrasting to the cells treated with **T2**. The cellular uptake is also dose dependent for compound **B1**. However, the relative concentration of intracellular molybdenum is very low as compared to the administered molybdenum in complexes; in the case of **B1** there is less than 0.005 μmol of Mo/million cells, which corresponds to less than 0.5% of the administered molybdenum. In opposition, raising concentrations of **T2** do not seem to be directly related to the intracellular molybdenum content. These results may explain the antitumoral potency of each compound when compared with each other, as **B1** showed a stronger cytotoxicity effect than **T2** (Table 3).

3.5. Octanol/water partition coefficient

Preliminary studies on the partition coefficients, *P*, were carried out to estimate how easily the compounds **T2** and **B1** are able to pass through a biological membrane. The *P* measurements are based on the difference in solubility that a given compound exhibits in an aqueous vs. a hydrophobic medium [39]. Complex **B1** presented a hydrophobic behavior (log $P = 0.760 \pm 0.039$), which is consistent with the high levels of intracellular molybdenum detected through cellular uptake studies. In what concerns compound **T2**, it was not possible to determine a conclusive value of log *P*. However, preliminary studies indicated that it possesses a less hydrophobic nature than **B1**, which would be in agreement with its cellular uptake results.

3.6. Absorption titration

Electronic absorption spectroscopy is universally employed to study the binding mode of DNA to complexes [40]. The absorption spectra of **T2** in the absence and presence of ct DNA are shown in Fig. 6. The addition of ct DNA (0–50 μM bp^{-1}) to **T2** led to spectral changes with hyperchromism of the 299 nm band. For the absorbance data at 299 nm, a plot of $D/\Delta\varepsilon_{ap}$ vs. *D* is shown in the inset of Fig. 6. This plot indicates that there is a linear relationship, with a binding constant value (*K*) of 2.08 (±0.98) × 10^5 M^{-1}. The binding of **B1** to ct DNA also led to similar spectral changes, with hyperchromism of the 272 nm absorption band. The *K* value for **B1** was calculated to be 3.68 (±2.01) × 10^5 M^{-1}.

The results indicate that the complex **T2** binds more strongly than **B1**. However, both *K* values are lower than the observed for ethidium

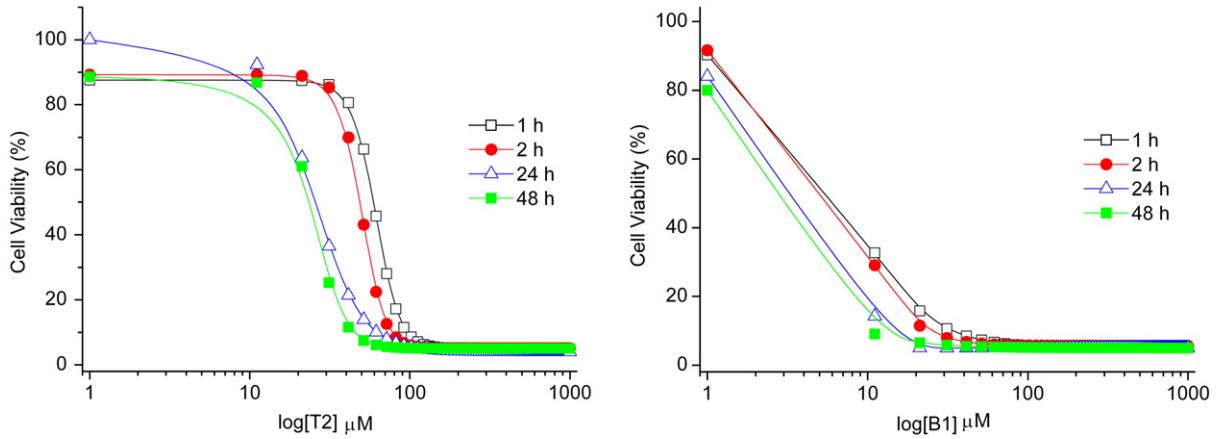

Fig. 4. Treatment time dependence of the cytotoxicity of **T2** and **B1**, respectively. The arrow indicates the variation of cell viability with the increasing incubation time.

bromide ($K_{EthBr} = 1.4 \times 10^6\ M^{-1}$), a typical classical intercalator [41]. Nevertheless, it is possible that intercalation with DNA might be one of the binding patterns, since the tested molybdenum complexes contain aromatic ligands (1,10-phenanthroline on **B1** and 2,2′-bipyridyl on **T2**) with extended π systems, which could intercalate in DNA [42].

3.7. Conclusions

Five molybdenum(II) and one tungsten(II) complexes were synthesized and tested for their cytotoxicity against HeLa, MCF-7, and N1E-115 cell lines *in vitro*. These complexes revealed to be very effective, exhibiting activities with IC_{50} values ranging from 3 to 45 μM. Two different molybdenum complexes, **T2** and **B1**, showed that maximum cytotoxic effect is established after 24 h of drug exposure time. The intracellular molybdenum uptake occurs differently for these two complexes, with uptake being dependent of increasing drug concentration for **B1**, contrarily to **T2**. Accordingly, complex **B1** displayed a hydrophobic behavior with a log *P* of 0.760 ± 0.039, suggesting that **B1** might be able to pass more easily through a biological membrane. The binding interactions of **B1** and **T2** with ct DNA could be assigned to intercalation, in agreement with their spectral changes (modest hyperchromicity). The binding constants are 2.08 (±0.98) × 10^5 and 3.68 (±2.01) × $10^5\ M^{-1}$, at 37 °C, for **T2** and **B1**, respectively, these values being lower than the one determined for the classical intercalator, ethidium bromide. Future work will address the intracellular localization of molybdenum, further studies with DNA molecules and other physical determination in order to obtain a clear understanding of the mechanism of action of these molybdenum compounds as they might prove to be of application in target-based cancer therapy.

Abbreviations

IC_{50}	inhibitory concentration (dose causing 50% inhibition of cell growth)
bpy	2,2′-bipyridyl
phen	1,10-phenanthroline
ct DNA	calf thymus DNA
MTT	3-(4,5-dimethylthiazol-2-yl)-2,5-diphenyltetrazolium bromide
DMEM	Dulbecco's Modified Eagle's medium
RPMI	Royal Park Memorial Institute
ICP-MS	inductively coupled plasma mass spectrometry
fac	facial
FBS	fetal bovine serum

Table 4
Cytotoxicities of compounds studied as measured by the MTT assay in HeLa cells.

Compounds	IC_{50} (μM)			
	After 1 h	After 2 h	After 24 h	After 48 h
T2	54	42	18	18
B1	5	3	1	1

Acknowledgements

The authors are grateful to F. Antunes (FCUL) for providing the cell lines and to F. Martins (FCUL) for inestimable help in octanol partition studies. The authors thank the Portuguese National Mass Spectrometry Network (REDE/1501/REM/2005). MSS (SFRH/BD/48640/2008) thanks FCT for a research grant.

Appendix A. Supplementary data

Supplementary data associated with this article can be found, in the online version, at doi:10.1016/j.jinorgbio.2010.07.006.

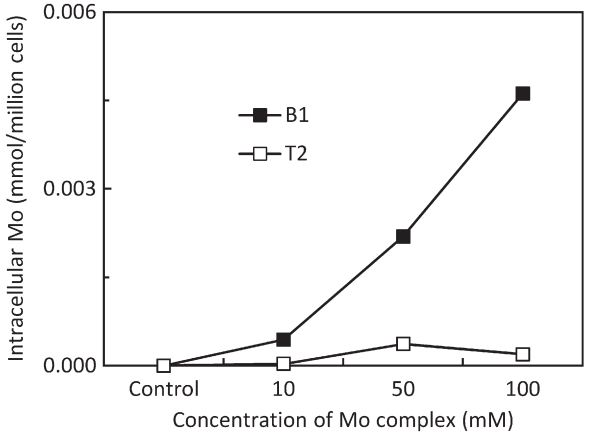

Fig. 5. Comparison of the intracellular molybdenum concentration in HeLa cells after 48 h of exposure to compounds **T2** and **B1**.

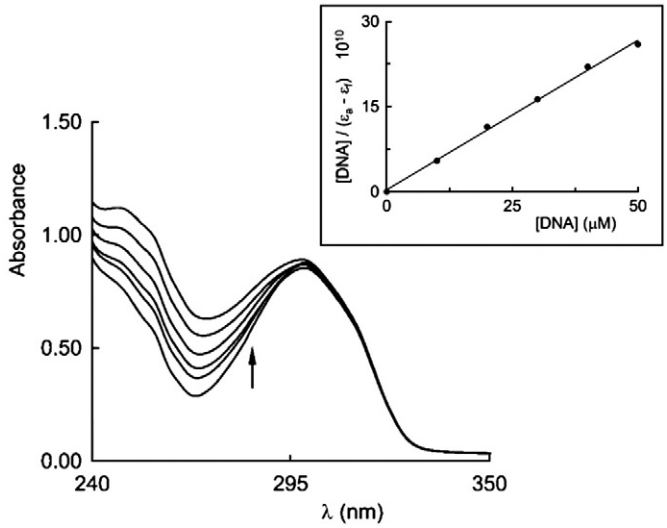

Fig. 6. UV–Vis absorption spectra of **T2** (20 μM) in Tris buffer in the presence of increasing amounts of ct DNA [DNA] = 0, 10, 20, 30, 40, and 50 μM. The arrow indicates the absorbance changes upon increasing DNA concentration. The inset is a plot of $D/\Delta\varepsilon_{ap}$ vs. D for the titration of DNA to complex. Absorbance was monitored at 299 nm.

References

[1] C. Thurier, P. Doppelt, Coord Chem Rev 252 (2008) 155–169.
[2] V.A. Friese, D.G. Kurth, Coord Chem Rev 252 (2008) 199–211.
[3] M.W. Cooke, D. Chartrand, G.S. Hanan, Coord Chem Rev 252 (2008) 903–921.
[4] K.H. Thompson, C. Orvig, Dalton Trans (2006) 761–764.
[5] T. Storr, K.H. Thompson, C. Orvig, Chem Soc Rev 35 (2006) 534–544.
[6] V. Ritleng, M.J. Chetcuti, Chem Rev 107 (2007) 797–858.
[7] L. Yin, J. Liebscher, Chem Rev 107 (2007) 133–173.
[8] K.R. Harrap, Cancer Treat Rev supl A (1985) 21–33.
[9] H. Köpf, P. Köpf-Maier, Angew Chem Int Ed 18 (1979) 477–478.
[10] M.M. Harding, G. Mokdsi, Curr Med Chem 7 (2000) 1289–1303.
[11] P. Ghosh, O.J. D'Cruz, R.K. Narla, F.M. Uckun, Cancer Res 6 (4) (2000) 1536–1545.
[12] P. Köpf-Maier, T.J. Klapötke, Cancer Chemother Pharmacol 29 (1992) 361–366.
[13] P. Köpf-Maier, T.J. Klapötke, Cancer Res Clin Oncol 118 (1992) 216–221.
[14] P. Köpf-Maier, H. Köpf, E.W. Neuse, J Cancer Res Clin Oncol 108 (1984) 336–340.
[15] X.M. Luo, H.J. Wei, S.P. Yang, J Natl Cancer Inst 71 (1983) 75.
[16] H. Wei, X. Luo, X. Yang, Chan Abstr 108 (1988) 1995.
[17] European patent, 1988, application number 88905227.0.
[18] H. Fujita, T. Fujita, T. Sakurai, T. Yamase, Y. Seto, J Exp Med 168 (1992) 421–426.
[19] I.H. Hall, C.B. Lackey, T.D. Kistler, R.W. Durham, J.M. Russell, R.N. Grimes, Anticancer Res 20 (2000) 4245–4254.
[20] L. Shuncheng, L. Xiaoming, C. Jingrong, patent number CN1321644, 14/11/2001.
[21] M.R. Matos, C.C. Romão, C.L. Pereira, S.S. Rodrigues, M. Mora, M.P. Silva, P.M. Alves, C.A. Reis (2005) Patent WO/2005/087783.
[22] C. Kisker, H. Schindelin, D.C. Rees, Annu Rev Biochem 66 (1997) 233–267.
[23] S. Quintal, J. Matos, I. Fonseca, V. Félix, M.G.B. Drew, N. Trindade, M. Meireles, M.J. Calhorda, Inorg Chim Acta 361 (2008) 1584–1596.
[24] (a) H. Tamura, M. Miwa, Chem Lett (1997) 1177;
(b) D. Osella, M. Ferrali, P. Zanello, F. Laschi, M. Fontani, C. Nervi, G. Cavigiolo, Inorg Chim Acta 306 (2000) 42;
(c) L.V. Popova, V.N. Babin, Y.A. Beleusov, Y.S. Nekrasov, A.E. Snegireva, N.P. Borodina, G.M. Shaposhnikova, O.B. Bychenko, P.M. Raevskii, M.N. Morozova, A.I. Ilyna, K.G. Shitkov, Appl Organomet Chem 7 (1993) 85;
(d) L.V. Snegur, A.A. Simenel, Y.S. Nekrasov, E.A. Morozova, Z.A. Starikova, S.M. Peregudova, Y.V. Kuzmenko, V.N. Babin, L.A. Ostrovskaya, N.V. Bluchterova, M.M. Fomina, J Organomet Chem 689 (2004) 2473;
(e) V.N. Babin, P.M. Raevskii, K.G. Snchitkov, L.V. Snegur, Y.S. Nekrasov, Mendeleev Chem J (1995) 39.
[25] M.S. Saraiva, S. Quintal, F.C.M. Portugal, T.A. Lopes, V. Félix, J.M. Nogueira, M. Meireles, M.G.B. Drew, M.J. Calhorda, J Organomet Chem 693 (2008) 3411–3418.
[26] H. tom Dieck, H. Friedel, J Organomet Chem 14 (1968) 375–385.
[27] A.T.T. Hsieh, B.O. West, J Organomet Chem 112 (1976) 285–296.
[28] G.M. Sheldrick, Acta Cryst A64 (2008) 112–122.
[29] A.L. Spek, PLATON, A Multipurpose Crystallographic Tool, Utrecht University, Utrecht, The Netherlands, 2005.
[30] T. Mossman, J Immunol Meth 65 (1983) 55–63.
[31] J.B. Waern, C.T. Dillon, M.M. Harding, J Med Chem 48 (2005) 2093–2099.
[32] D. Ma, C. Che, F. Siu, M. Yang, K. Wong, Inorg Chem 46 (2007) 740–749.
[33] F. Chen, P. Yang, C. Chen, G. Lee, S. Peng, J Organomet Chem 693 (2008) 537–545.
[34] J. Perez, L. Riera, V. Riera, S. Garcia-Granda, E. Garcia-Rodriguez, J Am Chem Soc 123 (2001) 7469–7470.
[35] P.M.F.J. Costa, M. Mora, M.J. Calhorda, V. Félix, P. Ferreira, M.G.B. Drew, H. Wadepohl, J Organomet Chem 687 (2003) 57-/68.
[36] J.R. Ascenso, C.G. de Azevedo, M.J. Calhorda, M.A.A.F. de, C.T. Carrondo, P. Costa, A.R. Dias, M.G.B. Drew, V. Félix, A.M. Galvão, C.C. Romão, J Organomet Chem 632 (2001) 197–208.
[37] A. Romerosa, P. Bergamini, V. Bertolasi, A. Canella, M. Cattabriga, R. Gavioli, S. Manas, N. Mantovani, L. Pellacani, Inorg Chem 43 (2004) 905–913.
[38] D.L. Ma, C.M. Che, Chem Eur J 9 (2003) 6133–6144.
[39] L.P. Graham, An Introduction to Medicinal Chemistry, Oxford University Press, Oxford, UK, 1995.
[40] J.M. Kelly, M.J. Murphy, D.J. Mcconnell, C. Ohuigin, Nucleic Acids Res 13 (1985) 167–184.
[41] S. Ramakrishnan, V. Rajendiran, M. Palaniandavar, V.S. Periasamy, B.S. Srinag, H. Krishnamurthy, M.A. Akbarsha, Inorg Chem 48 (2009) 1309–1322.
[42] R.S. Kumar, S. Arunachalam, V.S. Periasamy, C.P. Preethy, A. Riyasdeen, M.A. Akbarsha, Eur J Med Chem 43 (2008) 2082–2091.